Pollution, 6(2): 267-284, Spring 2020
DOI: 10.22059/poll.2019.290078.690
Print ISSN: 2383-451X Online ISSN: 2383-4501
Web Page: https://jpoll.ut.ac.ir, Email: jpoll@ut.ac.ir

A Review of Air Pollution and Solutions Way Management Related to Ribbed Smoked Sheets (RSS) Production of Community-Level Rubber Cooperatives in Thailand: Smoke, Soot and PAHs particles

Kalasee, W. * and Teekapakvisit, C.

King Mongkut's Institute of Technology Ladkrabang, Prince of Chumphon Campus, 17/1 M.6 Pathiu District, Chumphon 86160, Thailand

Received: 03.10.2019 Accepted: 18.02.2020

ABSTRACT: In Thailand, RSS chamber of community-level rubber cooperatives can be classified into two models: old and new model, named after the years of their establishment. Hot gas as a heat supply from Para-rubber (PR) wood *(Hevea brasiliensis)* combustion is used for removing moisture from the natural rubber (NR) sheets. Smoke and soot particles from PR wood burning has effected to the quality of the NR sheet and the pollution in the workplace area and lead to health problems of the worker. Cascade impactors are equipment for measuring the smoke and soot particles size distribution from PR wood combustion. PAHs compounds from PR wood combustion were found 15 different PAHs components (Tekasakul et al., 2005; Furuuchi et al., 2006). Important methods in decreasing smoke and soot particles from combustion of PR wood for rubber smoking chamber are separation equipment and ventilation designed by computational fluid dynamics (CFD) technique. In this article, the separation method is focused on smoke and soot particle collection to maintain the quality of the NR sheet. This equipment is reviewed both indoor and outdoor, for example, an impaction wall, electrostatic precipitator, stainless-wire, etc. This review indicates that the ESP installing between the furnace and the smoking chamber is suitable to eliminate aerosol particles at the rubber smoking industry. In addition, CFD technique reports is aimed at collecting aerosol particles for decreasing smoke and soot particles emission from rubber smoking chamber is presented.

Keywords: Para-Rubber; wood combustion; Filtration; ESP; CFD.

INTRODUCTION

Smoke, soot and polycyclic aromatic hydrocarbons (PAHs) are produced by biomass burning of dried and cured the agriculture product (Ravindra et al., 2006; Wang et al., 2010), for example, ribbed smoked sheet (RSS). They were resulted from the carbonaceous materials combustion (Kalasee et al., 2003; Deng et al., 2006).

In Southeast Asian countries, especially Thailand, PR wood has been immensely used in multitudinous industries (Promtong & Tekasakul, 2007; Kalasee, 2009; Chaivatamaset, 2015). Incomplete combustion of PR wood results in the great emission of particles; smoke and soot; (Furuuchi et al., 2006; Phairuang et al., 2019) and chemical compositions such as PAHs (Chomanee et al., 2009; Keyte et al., 2013; Hata et al., 2014; Chaivatamaset, 2015).

Thailand is the biggest natural rubber

* Corresponding Author, Email: arwkalasee@gmail.com

(NR) production and exportation country in Southeast Asian and the world. In year 2016, Thailand produced natural rubber about 37.5% of the total world production or about 4.5 million tons (Thailand Rubber Research Institute, 2017). More than 85% of NR products of Thailand are exported to China, Japan, USA and India. Generally, NR products include vehicle tires, toys, condoms, medical gloves (Kalasee, 2009; Matiyanon et al., 2013; Rattanamechaiskul et al., 2016).

Currently in Thailand, More than 90% of NR products are RSS, rubber concentrated latex (RCL), and block rubber (Thailand Rubber Research Institute, 2018). Now, RSS and RCL consumption are increased in Thailand, Asia, and World. They are followed by increasing numbers of the automotive industry. In RSS process, the rubber sheets are washed and hung on bamboo bars to dry in the smoking chambers. Hot gas production from Para rubber wood combustion is flowing to the rubber in smoking chamber via the tunnel which is constructed under the floor of the chamber. When the wood is burned, the ash, carbon, water vapor, smoke and soot particles are produced. Smoke and soot particles from wood combustion affect to the workplace environment and can cause the worker's health problem. Study on the characteristics of smoke and soot particles is necessary. The important characteristics of the study are the physical and chemical properties. The physical properties of smoke and soot particles from Para rubber wood combustion can be divided into two characteristics; particles size distribution and particles mass concentration. The chemical characteristics of smoke and soot particles from Para rubber wood combustion related mainly to chemical constituents of particles such as PAHs and organic compounds. For the smoke and soot particles collection apparatuses, three techniques (filtration by stainless-wire mesh, inertial impaction (impaction wall) and electrostatic precipitator) are appropriate to use in the rubber smoking chambers (Tantichaowanan, 2005; Tekasakul et al., 2005; Tekasakul et al., 2006; Kalasee, 2009; Ruttanachot, et al., 2011).

Recently, CFD technique is used to decrease smoke and soot particles emissions from the rubber smoking chamber to environment. The modified ventilation system which uses CFD technique simulation and experiment is in good agreement. Smoke and soot particles ventilation would be pleasurably improved by appropriate roof ridge exit (Purba, 2009; Purba & Tekasakul, 2012). Thus, this review article focuses on the discussion of air pollutants (smoke, soot and PAHs) from PR wood combustion in a NR sheet smoking process and the different techniques to decrease this effect.

Ribbed Smoked Sheets Chamber

Ribbed smoked sheets (RSS) chamber of community-level rubber cooperatives in Thailand can be classified into two models (old and new model), named after the years of their establishment. The old model so-called model 1994 contains seven rubber smoking chambers and each chamber has capacity 1.2-2.0 ton on a dried basis (Kalasee et al., 2003; Promtong, 2006; Choosong et al., 2010). The new model established in 1995. This model contains four rubber smoking chambers and the capacity of each chamber is double of the old chamber model capacity. The old chamber model has dimensions of 2.6 m width, 6.2 m length, and 3.7 m height. It is constructed of brick, mortar and cement. A steel gate is built in the front wall for loading and unloading rubber. At the ceiling of chamber, it has two ventilating windows. Furnace is located at 0.5 m below the floor and it is constructed in the rear of the chamber. Heat distributing tunnels have 4 inch diameter and are built in twelve positions at the floor level of the room. The bamboo bars are used to hang the rubber sheets on a steel crate which has dimensions of 2.0 m width, 2.0 m length, and 2.0 m height. The old model can contain three crates, but the new model can contain six crates. PR woods consumption is about 0.8-1.2 ton per ton of dried products both old and new chambers (Kalasee, 2009; Choosong et al., 2010).

RSS Production Process and Monthly RSS Production Changes

In the RSS production process**,** the raw material or fresh para-rubber latex; white liquid; is tapped and collected from Para-rubber tree. The membered farmers of rubber cooperative transport this latex to the RSS factory during 7 A.M.-11 A.M (Choosong et al., 2010; Kalasee et al., 2012; Matiyanon et al., 2014; Rattanamechaiskul et al., 2016). During 8 A.M.-12.00 A.M., this latex is poured to tanks which are located near the chamber. Until 2 P.M. water and the acid such as formic and acetic is added to para-rubber latex. Aluminum spacers are immersed in this latex and used as partitions to produce sliced slabs (around 3 cm × 50 cm × 50 cm) of solidify the latex (tofu-like slabs). These slabs are then washed and squeezed to form thin layer sheets which have a thickness about 3-4 mm by a squeezing machine. Theses sheets are hung on the bamboo bars which placed at steel crate by the worker before they are transferred to dry in a smoke chamber. During the high season (December to February), the capacity of the factory is more than 15000 sheets per week and it has capacity about 7000-11000 sheets per week during June to September (moderate season). This production is the lowest during the deciduous fall season (March to May) because the most of farmers stopped to tap the para-rubber trees (Choosong et al., 2010).

Particles Distribution and Particles Sampling Method

Combustion particles from Para rubber wood burning can be divided into two groups (primary and secondary particles). In the combustion zone, the primary form of combustion particles is occurred at high temperature and the second form of particles is discovering in the fuel gas, chamber, chimney and atmosphere.

The measurement of smoke and soot particles distribution from para-rubber wood burning appliances is very challenging. Many reports show that particles emissions from wood combustion on two main factors. The first is particles size distribution and the second is mass concentration.

The particles size distribution measures an aerosol size that can be superseded by diameter (Friedlander, 2000; Butler & Mulholland, 2004; Riahi et al., 2013). According to Giechaskiel et al. (2014) report, the particle size is determined based on characteristics, e.g. inertia, optical properties.

Cascade impactors are apparatuses for measuring the particles size distribution in mass that operates based on the categorization of inertial of aerosol particles (Davies, 1966; Hinds, 1999). They are the most appropriate equipment to achieve the air quality measurements. These reports are described in both the European (Alonso et al., 2017; Kesavan et al., 2017), Asian (Cheng et al., 2007) and Australian (Gras & Michael, 1979). The testing method is set in STP555, STP1002 and STP1287.

One type apparatus of cascade impactors is Andersen air sampler (Andersen, 1956; Cheng et al., 2007; Hata et al., 2014; Alonso et al., 2017; Kesavan et al., 2017). The Andersen sampler operates on the principle of inertial impaction. In each stage, the sampler consists of a plate for collection surface and specification of nozzle arrangement. The sample air is flowed into the sampler through stage by stage. The total nozzle area and nozzle size decrease with the stage from upstream to downstream. After the particles pass through a nozzle, the particles that have diameter smaller than a cut-off diameter of stage remain in the air stream sample and pass onto the next stage. But the larger particles that have much sufficient inertia are collected at plate or collection surface. In the analysis, the stage cut-off diameter or d_{50} is defined as the aerodynamic diameter at 50% cumulative oversize percentage of particles. It is used to find the size distribution of particles which is known as the mass median aerodynamics diameter (MMAD). The geometric standard deviation (GSD) of the particles is defined as (Hinds, 1999):

$$GSD = \frac{d_{84.1\%}}{d_{50\%}} = \frac{d_{50\%}}{d_{15.9\%}} = [\frac{d_{84.1\%}}{d_{15.9\%}}]^{1/2} \qquad (1)$$

where $d_{15.9}$, d_{50} and $d_{84.1}$ are the diameters where cumulative oversize percentage of particles are 15.9, 50 and 84.1, respectively.

The normally used technique for appraisal particulate mass concentrations relates to filtration (Davies, 1966; Hinds, 1999; Murry, 2000; Letts et al., 2003). Under controlled relative humidity and temperature conditions, filters are weighed before and after testing. Particles mass concentrations are calculated from the volume of gas sampled and the filter mass increase.

In this section, the study of smoke and soot particle characteristics from Para rubber wood combustion is reviewed. Many reports of researchers are discussed as follows.

Kalasee et al. (2003) is the first report to study on smoke and soot particles distribution from para-rubber wood combustion. The report showed that the smoke and soot particles size distribution was measured by an 8-stage cascade (Andersen) sampler. Studied by Kalasee et al. (2003), the particles size distribution was a single-model behavior. MMAD and GSD of smoke and soot particles were found to be 0.95 micron and 2.51, respectively. The moisture content of the Para rubber wood had effected on the mass concentration of the smoke and soot particles. The result also showed that the PR wood samples had moisture content ranging from 34.75 to 107.5% dry basis and the mass concentration of their combustion were 47 to 1358 mg/m^3.

Investigated by Furuuchi et al. (2006), the characteristics of smoke and soot particles from the Para rubber wood combustion had an impact on the workplace environment. Their results of the smoke and soot particles size distribution agreed with of Kalasee et al., 2003 report. For inside the workplace, their result showed that the particles concentration was 0.33 mg/m^3 and it was higher than the acceptable limit by the Thailand Department of Pollution Control.

In 2009, the study of Chomanee et al. showed that the smoke and soot particles size distribution was similar to the results from Kalasee et al. (2003). In their experiment, the air sampler was improved to prevent its condensation. Their report showed that MMAD and GSD are found to be 0.68 micron and 3.04, respectively.

The studies of Hata et al. (2014) presented that the characteristics of particles emitted from the Para rubber wood burning in a laboratory-scale (tubular electric furnace). Their results showed that the increase of the heating rate had a relative influence to an increase of the total particles mass concentration emissions from the Para rubber wood combustion. For the graph relation between cumulative mass fraction and aerodynamic diameter of the particles distribution from para-rubber wood burning in their results indicated that MMAD and GSD were found to be about 0.7 micron and 2.6, respectively. Their result was similar to the results from Kalasee et al., (2003); Chomanee et al., (2009).

PAHs Concentration

PAHs are organic compounds that consisted of hydrogen and carbon atoms (Venkataraman et al., 2002; Tang et al., 2005; Choosong et al., 2007, Salaudeen et al., 2017). PAHs have toxic effects on the function of cellular membranes (Fang et al., 2004; Adeola et al., 2007; Amuda & Imeokparia, 2007) and can cause human's health problems, e.g. cancer. PAHs are emitted to an ambient air primarily from the incomplete of fuel combustion, for example, petroleum (Bharti et al., 2019; Motamedimehr et al., 2019) and wood (Tekasakul et al., 2008; Chomanee et al., 2009; Choosong et al., 2010; Hata et al., 2014). Many reports are shown that the PAHs are precursors of smoke and soot particle nuclei. Homann & Wagner (1966) and many researchers (Martinis et al., 2002; Venkataraman et al., 2002; Saez et al., 2003; Chao et al., 2008; Croft et al., 2016) studied on PAHs components from an acetylene-oxygen diffusion flame and their results showed that PAHs had two types of poly-aromatic (PA) molecules. The first type of PA molecular is compounds without side chain (acenaphthalene, naphthalene, phenanthrene and coronene) and the second one is PA compounds which have molecular weight of 150-500 or with side chain (Shin et al., 1988; Simonelt et al., 1991; Fenklach & Wang 1991; Salaudeen et al., 2017; Mahmudi et al., 2019; Bharti et al., 2019).

In this section, the reviewer studied PAHs concentration from Para rubber wood combustion. Many reports are discussed as follows.

Tekasakul et al. (2005) and Furuuchi et al. (2006) showed that 15 different PAHs components from the Para rubber wood combustion are found in the aerosol particles and ambient air at the workplace of RSS factory.

The report of Furuuchi et al. (2006) showed that the total PAHs particles concentration from Para-rubber wood combustion was very high. For the soot particle size larger than 3.3 micron, the PAHs concentrations were smaller than 10^3 ng/m^3 while the concentration for smaller particles was about 10^5 ng/m^3.

The report of Bai et al. (2007) showed that soot particles from Para rubber wood burning had a single modal size distribution. The decomposition of PAHs particles from the rubber-woods combustion happening using Soft X-rays with a wave length of 1.3×10^{-4} to 4.1×10^{-4} micron. The increased total energy of soft X-rays had a relative influence to increase the effective decomposition of PAHs particles.

Tekasakul et al. (2008) presented that the size distribution of PAHs particles from Para rubber wood combustion in ambient air around the rubber smoking factory had a single-model behavior. During the dry season, PAHs concentration in ambient air was higher than their concentration during the rainy season.

Chomanee et al. (2009) presented that sixteen PAHs compounds from Para rubber wood combustion were able to be classified in two types: 2-3 rings and 4-6 rings. Naphthalene, Acenaphthylene, Acenaphthene, Fluorene, Phenanthrene and Anthracene are 2-3 rings of PAHs compounds, while the 4-6 rings PAHs are Fluoranthene, Pyrene, Benz[a]anthracene, Chrysene, Benzo[b]fluoranthene, Benzo[k]fluoranthene, Benzo[a]pyrene, Indeno[1,2,3-cd]pyrene, Dibenz[a,h] anthracene, and Benzo[g,h,i]perylene. The increasing of time period of combustion has a relative influence to decrease PAHs concentration.

Investigated by Choosong et al. (2010), the authors illustrated that wind direction, seasonal changes, the geometry of the oven and rubber smoking chamber building and ventilation type has a relative influence to change the particulate and PAHs concentrations from Para rubber wood combustion. This report also depicted that PAHs concentrations in the ventilation zone was higher than their concentrations in the workplace.

The report of Hata et al. (2014) had shown that the heating rate and the combustion temperature had a significant effect on PAH emissions. The soot particles from Para rubber wood combustion that was smaller than 0.43 micron made a large contribution to PAHs.

Particles Collection Method

Now, there have been many techniques to catch the little particles, for example, filtration, cyclones separation, gravitational settling, etc. However, the major techniques are requiring a large space for installation. The rubber smoking chamber is the wet areas. So, the installing various particles collection apparatuses is constrained. The major reports show that there are only three techniques; filtration by stainless-wire mesh (ASTM E11 & ISO 3310-1: 2016), inertial impaction (impaction wall) and electrostatic precipitator (JB/T 12591-2016); which appropriates for using at the rubber smoking chambers (Kalasee et al., 2003; Docherty et al., 2005; Tantichaowanan, 2005; Kalasee, 2009; Ruttanachot, et al., 2011).

Filtration by Stainless-Wire Mesh

Because filtration by filters is simple to use and effective, it is the most interest particles collection technology in the present. Therefore many researchers have studied appropriate filter materials for removing smoke and soot particles from wood combustion for filtration method. Large particles from the Para rubber wood burning are collected by a stainless-wire mesh by inertial impaction method at a high velocity while the small particles are removed from hot gas by Brownian diffusion method (Sippola, 2002; Kalasee, 2009; Sippola & Nazaroff, 2010). The parameters involved in Brownian diffusion and inertial impaction are Peclet number (*Pec*) and Stokes number (*Stk*). Where u_f is the filtration velocity, d_{ws} is the stainless-wire mesh diameter, and D_B is the particle Brownian diffusivity. Thus, Peclet number (*Pec*) is given by

$$Pec = \frac{u_f d_{ws}}{D_B} \qquad (2)$$

The collection efficiency of a filter decreases when the *Pec* increases and the *Stk* decreases. Thus, Stokes number (*Stk*) can be defined as (Hinds, 1999)

$$Stk = \frac{\rho D_p^2 u_f C}{9\mu d_{ws}} \qquad (3)$$

where ρ is particle density, D_p is particle diameter, C is Cunningham slip correction factor, and μ is viscosity (Davies, 1966; Hinds, 1999).

During working period, the pressure drop increasing has a relative influence to decrease the filter (mesh) collection efficiency (Letts et al., 2003). Thus, the pressure drop across filters (ΔP) can be defined as (Davies, 1952):

$$\Delta P = \frac{\mu_g u_{vg} F_t}{d_{ws}^2}\left[64F_s^{1.5}\left(1+56F_s^3\right)\right] \qquad (4)$$

In this equation, μ_g is the gas viscosity, uv_g is the face gas velocity, F_t is the thickness of filter, and F_s is the filter packing density.

Studied by Kalasee (2003), the author showed that the plate of mesh #200 wires-stainless is installed on the frame above the floor of the rubber smoking chamber. This report showed that the particles collection efficiency of this apparatus is about 50% and the pressure drop is higher than 200 Pa at an initial velocity value of 28 cm/s. The results of this report were similar to the results from Sirisantipong & Tantichaowanan (2002).

Inertial Impaction

Inertial impaction or impaction wall is an uncomplicated particle collection technique. For the rubber smoking factory, the flat plate is installed in the tunnel between a furnace and the rubber smoking chamber. The principle of this technique is the large particles which are unable to pass through a nozzle. These particles are clashed with a flat plate because they have too many the inertial forces (Hinds, 1999; Kalasee, 2009).

According to the method, the dimensionless number which is described to the behavior of particles suspended in airflow is Stokes number (*Stk*) and it can be defined as (Hinds, 1999)

$$Stk = \frac{\rho D_p^2 UC}{9\mu W} \tag{5}$$

In this equation, *U* is an air velocity in throat, and *W* is a width of throat. The slip correction factor can be calculated from (Hinds, 1999)

$$C = 1 + \frac{D_p}{\lambda}(2.34 + 1.05e^{-(\frac{0.390\lambda}{D_p})}) \tag{6}$$

This equation should be placed when *C* appears first time and λ is a mean free path in air molecule.

Studied by Kalasee (2009), the apparatus (inertial impaction or impaction wall) in his research was a flat zinc plate. A plate was installed in the tunnel between a stove and the rubber smoking room. This report showed that the soot particles from para-rubber wood combustion size in 3.3 to 4.7 micron size range were caught by a flat zinc plate. The impaction system was shown in Fig. 1. In this system, the impaction wall has the length (l_{iw}) of 150 cm and height (h_{iw})of 60 cm. A hot gas flow in the throat tunnel (stopping distance) was like as a rectangular acceleration nozzle. The length (l_{th}) and width (W_{th}) of this throat were 30 cm and 60 cm, respectively. The stopping distance (S_d) was 30 cm. The ratio of S_d / w_{th} was 0.5. Hence, the value of Stokes number in theory for the stopping distance was 0.5 (Hinds, 1999). The range of velocity values of hot gas flowing in this throat tunnel was 200-500 cm/s. The result of this report showed that the dust-loading had no influence to the collection efficiency and it was similar to the results from Phonchat & Choowijit (2011).

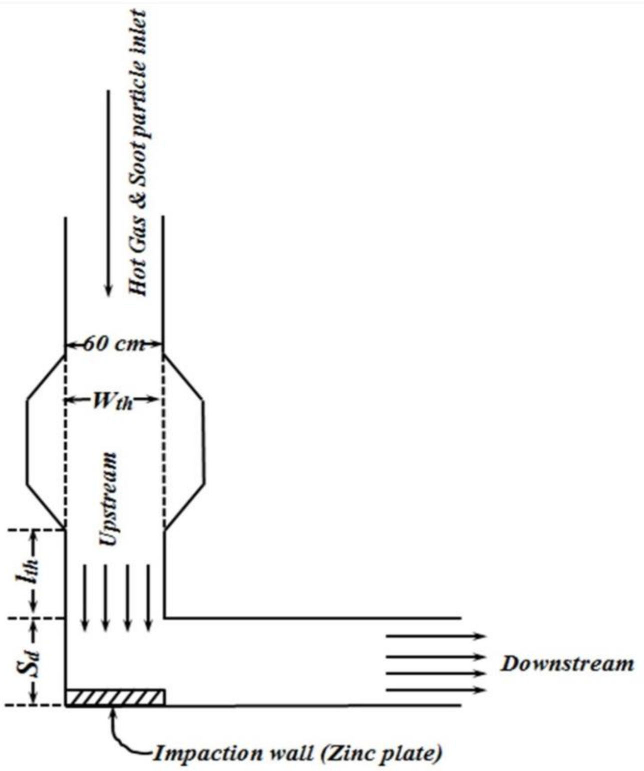

Fig. 1. Schematic diagram of the impaction system

Electrostatic Precipitator

Many researchers have proposed many methods to improve the collection efficiency of electrostatic precipitator (ESP) and electrode cleaning mechanisms for removal of soot particles from wood combustion (Kalasee et al., 2003; Intra et al., 2005; Kocik et al., 2005; Tantichaowanan, 2005; Tekasakul et al., 2005; Tekasakul et al., 2006; Intra et al., 2007; Kalasee 2009; Intra et al., 2010; Lin et al., 2011; Ruttanachot et al., 2011; Ma et al., 2016; Lin et al., 2018). Firstly, ESP is installed in the 4 inch diameter tube which is built in twelve positions at the floor level of the room. ESP installation in the rubber smoking room is very dangerous because ESP works under an electric system, rubber smoking chamber has wetting area from rubber sheet dehydration and the knowledge of worker is rather low. Thus, ESP is installed in the tunnel between a furnace and the rubber smoking chamber in the present rather than installed ESP in the rubber smoking room.

ESP has high collecting efficiency for a small particles and its pressure drop is low (Kim & Lee, 1999; Tanaka, 2003; Tanaka, 2006; Long & Yao, 2010; Zhao et al., 2017). Collecting efficiency of ESP (μ) can be defined by using the Deutsch-Anderson equation (White, 1963; Kihm, 1987; Hinds, 1999).

$$\eta = 1 - \exp[\frac{-A_{cs}V_{pm}}{Q_g}] \tag{7}$$

In this equation, Q_g is the air flow rate, A_{cs} is the collection surface area, V_{pm} is the particle migration velocity, and it can be calculated from

$$V_e = \frac{q_e E_f C_s}{3\pi\mu_a D_p} \tag{8}$$

where E_f is the electric field strength, C_s is the slip correction factor, μ_a is the air viscosity, D_p is the particle diameter, and q_e is the particle charges, and it can be calculated from (Hinds, 1999)

$$q_e = ne \tag{9}$$

where e is the electrical charges, and n is the number of charge, and it can be calculated from (Hinds, 1999)

$$n = n_{fc} + n_{dc} \tag{10}$$

In this equation, n_{fc} is the number of field charging, and n_{dc} is the number of diffusion charging. White (1951) has been developing the equation of Fuchs (1947). In order to calculate the charging rate expression can be described by a differential equation of White (1951) as given by

$$\frac{dn_{dc}}{dt} = \pi r^2 C_i N_i . \exp(-K_{cc}\frac{n_{dc}e^2}{rkT}) \tag{11}$$

In this equation, t is the charging time, r is the particle radius, C_i is the average ion thermal velocity, $\underline{N_i}$ is the ion concentration, K_{cc} is Coulomb constant, k is Boltzmann constant, and T is the temperature. The integrated of the above equation can be given by

$$\int_0^{n_{dc}} \frac{dn_{dc}}{\exp(-K_{cc}\frac{n_{dc}e^2}{rkT})} = \int_0^t \pi r^2 C_i N_i dt \tag{12}$$

Thus, the number of diffusion charging (n_{dc}) caused by the diffusion charging time by the particle diameter (D_p) can be calculated from

$$n_{dc} = \frac{D_p kT}{2K_{cc}e^2}\ln\left[1 + \frac{\pi N_i t K_{cc} D_p C_i e^2}{2kT}\right] \tag{13}$$

For the number of field charging (n_{fc}), and it can be given by

$$n_{fc} = \left(\frac{3\alpha}{\alpha+2}\right)\left(\frac{D_p^2 E_f}{4K_{cc}e}\right)\left(\frac{\pi N_i t K_{cc} Z_i e}{1+\pi N_i t K_{cc} Z_i e}\right) \tag{14}$$

In this equation, α is the particle dielectric constant, and Z_i is the ion electrical mobility.

For the number of ion concentration (N_i), it can be given by (Intra & Tippayawong, 2011)

$$N_i = \frac{I_{ac} d_{ec}}{Z_i V_e \mu h t e} \tag{15}$$

In this equation, d_{ec} is the equivalent cylindrical radius, V_e is the voltage of discharge electrode, μ is the gas velocity, h is the height of the collection electrode, I_{ac} is the average corona current, and it can be given by

$$I_{ac} = \frac{\pi L h Z_i \alpha_0}{s^2 c \ln\left[\frac{d_{ec}}{r_0}\right]} \left(V_e\left[\left(V_e - V_c\right)\right]\right) \tag{16}$$

In this equation, L is the length of the collection electrode, α_0 is the free-space permittivity, V_c is the corona onset voltage, S is a half of the gap between collection electrodes, C is a half of the distance between wire electrodes, and r_0 is the radius of the discharge electrode.

For the equivalent cylindrical radius (d_{ec}), it can be given by (Parker, 1997)

$$d_{ac} = (2c)\left(0.18\exp\left[2.96\frac{s}{2c}\right]\right) \text{ For } 0.3 \le \frac{s}{2c} \le 1.0 \tag{17}$$

For the corona onset voltage (V_c), it can be given by

$$V_c = r_0 E_{oc} \ln\left[\frac{d_{ac}}{r_0}\right] \tag{18}$$

where E_{oc} is the corona onset electric field, and it can be given by

$$E_{oc} = \beta\left(32.2 + \frac{0.864x10^5}{\sqrt{r_0\beta}}\right) \tag{19}$$

where β is the density of gas.

In this section, the review of the study of the collecting efficiency of smoke and soot particle from Para rubber wood combustion by ESP is presented. The reports of researchers are discussed as follows.

Investigated by Tantichaowanan (2005) and Tekasakul et al. (2006), the authors had shown that the ESPs could be employed to remove smoke and soot particles from Para rubber wood combustion. In the laboratory, the ESPs were suitable for use at the high available voltage supply, which was constant at 15 kV. In a field experiment, the twelve ESPs units of their design were installed in the rubber smoking chamber and each of them was operated at 30 minute periods when the fresh PR wood was burned. The total time of the ESPs was operated about 10 hours and the collecting efficiency of the ESPs was higher than 40%.

In 2009, Kalasee proposed new ESPs to improve the design by Tantichaowanan (2005) and Tekasakul et al. (2006). In order to decrease the danger of the installation and usability, the ESPs are installed in the tunnel between a stove and the rubber smoking room. This report showed that ESPs were operated longer than 120 hours and the collecting efficiency of the ESPs was higher than 50%. The result was similar to the results from Kuarsakul et al. (2011).

The report of Kim et al. (2010) presented that CFD technique was appropriate to study and simulate the aerosol distribution in the ESP system. The recommendation of this report was shown that simulation of the galvanic field and space charge distributions of ESP system was designed by the change of plasma region.

An investigation by Ruttanachot et al. (2011) is improved ESPs technique of the earlier design by Kalasee (2009). Their ESPs contain fifteen collection plate electrodes. The cleaning system has water spray from a half of inch PVC pipes. The collecting efficiency of ESPs is higher than 60%. After ESPs was operated 120 minutes, the cleaning system is used to clean the collection plate electrodes for a life of ESP extending.

The report of Park et al. (2018) presented that the k–ε model (standard model of CFD technique) based on Finite Volume Method and the Lagrangian approach with the dynamic of particle charging were used to study the corona discharge model of ESP to solve the turbulent air flow and the motion and charging of aerosol particles in the ESP. This result showed that the differences in size, relative permittivity and density had the highest effect on the particle charging, the particle trajectory and the ESP collecting efficiency.

Computational Fluid Dynamics Technique

In the present, the CFD technique is utilized to investigate aerosol concentration, flow patterns, and particle motion (Loomans et al., 2002; Kanaoka et al., 2006; Zhang et al., 2006; Park et al., 2018; Rigopoulos, 2019). CFD methods can be divided into two major groups: accelerated methods and convention methods. The accelerated methods are then divided into two major groups: Hardware techniques and Advanced Numerical Methods. For convention methods, Finite Volume Method (FVM), Finite Difference Method (FDM), Finite Element Method (FEM), and Spectral Methods are the most popular methods. This methods are most highly accurate, widely used and normally tend to use in most of the commercial software packages, such as ANSYS CFX, FLUENT, FLOVENT, STAR-CD and FEMLAB.

The Navier-Stokes equations either in Lagrangian approach or in Eulerian are used to solve in most of the CFD methods (FVM, FDM, FEM and Spectral Methods). These equations are described in the conservation of mass, momentum and energy. However, some methods solve the Boltzmann equations instead of Navier-Stokes equations.

The continuity equation describing mass conservation for a steady incompressible flow can be given by

$$\frac{\partial}{\partial x_i}(\rho \overline{u_i}) = 0 \qquad (20)$$

where ρ is the density, $\overline{u_i^{'}}$ is the velocity fluctuation.

The differential equations for the conservation of momentum can be written as

$$\frac{\partial}{\partial x_i}(\rho \overline{u_i u_j}) = -\frac{\partial \overline{p}}{\partial x_i} + \frac{\partial}{\partial x_j} [\mu(\frac{\partial \overline{u_i}}{\partial x_j} + \frac{\partial \overline{u_j}}{\partial x_i}) - \rho \overline{u_i^{'} u_j^{'}}] - \rho g_i B(\overline{T} - \overline{T}_{ref}) \qquad (21)$$

where $\overline{u}$ is the mean velocity components (u, v, w), μ is the fluid viscosity. Here, x_i is the coordinate axis (x, y, z), g_i is the gravitational acceleration vector, $\overline{p}$ is the pressure, B is the thermal expansion coefficient, $\overline{T}$ is the mean temperature, and $\overline{T}_{ref}$ is the system surrounding temperature is used in work (the reference temperature).

The energy equation can be given by

$$\frac{\partial}{\partial x_i}(\rho \overline{u_i T}) = \frac{\partial}{\partial x_i}[\frac{\mu}{Pn}\frac{\partial \overline{T}}{\partial x_i} - \rho \overline{u_j^{'} T^{'}}] \qquad (22)$$

where Pn is the Prandtl number, $\overline{T^{'}}$ is the temperature fluctuation. The terms $-\rho \overline{u_i^{'} u_j^{'}}$ and $-\rho \overline{u_j^{'} T^{'}}$ are called the Reynolds stress (τ_{ij}) and the diffusion term for the enthalpy, respectively. The determination of these terms requires extra equations, which based on the proposed by Boussinesq (1877).

The standard k-ε model is the most widely used for modelling and simulation a variety of practical engineering flow. In this model, the kinetic energy of turbulence (k) equation is given by

$$\frac{\partial k}{\partial x_i}(\rho u_i) = \frac{\partial}{\partial x_i}[\frac{\partial k}{\partial x_i}(\mu + \frac{\mu_{tb}}{\sigma_k})] + S_p + B_p - \rho \varepsilon \qquad (23)$$

In the standard k-ε model, the dissipation rate (ε) equation is given by

$$\frac{\partial \varepsilon}{\partial x_i}(\rho u_i) = \frac{\partial}{\partial x_i}[\frac{\partial \varepsilon}{\partial x_i}(\mu + \frac{\mu_{tb}}{\sigma_\varepsilon})] + C_1 \frac{\varepsilon}{k}(S_p + C_2 B_p) - C_3 \rho \frac{\varepsilon^2}{k} \quad (24)$$

where μ_{tb} is the turbulent viscosity and it is calculated from

$$\mu_{tb} = \rho C_u \frac{k^2}{\varepsilon} \quad (25)$$

The model constants, proposed by Launder and Spalding (1974), are C_u= 0.09, C_1= 1.44, C_2= 1.0, C_3= 1.92, σ_k= 1.0 and σ_ε = 1.217, respectively.

In equation (23), $\rho\varepsilon$ is the destruction rate, S_p is the shear production and it is calculated from

$$S_p = \mu_{tb} \frac{\partial u_i}{\partial x_j}(\frac{\partial \overline{u_i}}{\partial x_j} + \frac{\partial \overline{u_i}}{\partial x_i}) \quad (26)$$

In equation (23), B_p is the buoyancy production term and it is calculated from

$$B_p = \mu_{tb} \frac{\partial u_i}{\partial x_j}(\frac{\partial \overline{u_i}}{\partial x_j} + \frac{\partial \overline{u_i}}{\partial x_i}) \quad (27)$$

In the presence of the theory involved in smoke aerosol particles transport, the only of particulate phase of smoke aerosol is a very small fraction (less than 0.0001%) of its total mass and volume. Bulk properties of smoke aerosol differ imperceptibly from those of pure air. So, one must adopt a microscopic point of view in the study of the properties of smoke aerosols (White, 1963; Kihm, 1987; Hinds, 1999).

By assuming smoke aerosol particle-laden air is a fluid with the density of air. Diffusion of smoke aerosol particles is determined by the convective diffusion equation and it is given by (Kanaoka et al., 2006)

$$\frac{\partial}{\partial t}\left(\rho_a M_f\right) + \frac{\partial}{\partial x_i}\left(\rho_a V_a M_f\right) = -\frac{\partial J_i}{\partial x_i} \quad (28)$$

In this equation, ρa is the density of air, M_f is the mass fraction of smoke aerosol particles, Va is the velocity of air, J_i is the local flux for i component, and it can be calculated from

$$J_i = \left(\frac{\mu_{tb}}{S_{ch}} + \rho_a D_{co}\right)\frac{\partial M_f}{\partial x_i} \quad (29)$$

where μ_{tb} is the turbulent viscosity, S_{ch} is the Schmidt number, and D_{co} is the diffusion coefficient.

When smoke aerosol particles flowing are assumed to be continuous. The trajectory of smoke aerosol particle can be known by representing them in the discrete phase The trajectory of particles phase is predicted by integration of the force balance on this particle, which is calculated by a Lagrangian frame of reference (Tian et al., 2007; Rigopoulos, 2010; Donde et al., 2013; Raman & Fox, 2016). This force balance equates the particle inertia with the forces acting on the particle. So, it can be presented for the x direction in the Cartesian coordinates, the force balance is calculated from

$$\frac{dV_{pi}}{dt} = F_{Di}\left(V_a - V_{pi}\right) + \frac{g_i\left(\rho_p - \rho_a\right)}{\rho_p} \quad (30)$$

where V_{pi} is the velocity of particle, g_i is the gravitational acceleration vector, ρ_p is the particle density, F_{Di} is the drag force, and it is calculated from

$$F_{Di} = \frac{3\mu_g \operatorname{Re} C_D}{4\rho_p D_p^2} \quad (31)$$

where μ_g is the velocity of air, D_p is the particle diameter, Re is the Reynolds number, C_D is drag efficiency, and it can be given by (Haider & Levenspiel, 1989)

$$C_D = \frac{24\left(1 + \beta_1 \operatorname{Re}^{\beta_2}\right)}{\operatorname{Re}} + \frac{\beta_3 \operatorname{Re}}{\beta_4 + \operatorname{Re}} \quad (32)$$

In this equation, β_1, β_2, β_3, and β_4 is the constant value and the Reynolds number (Re) is written as

$$\mathrm{Re} = \frac{\rho_a D_p \left| V_{pi} - V_a \right|}{\mu_g} \tag{33}$$

Lu et al. (1996) described the CFD technique using a single phase to represent the aerosol particle and air flow. Air continuity was used to calculate the set of equations for the control volumes and Lagrangian method was employed in the tracking model of particles.

Purba & Tekasakul (2012) presented that CFD technique was used to examine temperature, velocity, smoke and soot particles concentration, and particles trajectories in the rubber smoking chamber. The resulting figures such as pressure, temperature, particle path lines and streamline contours are also referred to the authors or the publication (Particulate Science and Technology). The high particles concentration occurred above the ceiling areas. However, the particles concentration was decreased along the height in a downward direction. The smoke and soot particles concentration was largely decreased by a modified ridge vents increasing at roof of the rubber smoking chamber.

The report of Dejchanchaiwong et al. (2017) has presented that a new rubber smoking chamber was constructed by the designed and simulated model of Tekasakul & Promtong (2008). The resulting figures; hot air velocity and temperature contours; are also referred to the authors or the publication (Applied Thermal Engineering). Although, the Para rubber wood consumption, the uniform temperature and hot air velocity, and reduction of drying time are the main objective of this research. But the indirect benefit of this research is the reduction of smoke and soot particles from Para rubber wood combustion by hot air reusing.

Recommendation of this review, CFD technique is very interesting method to improve the rubber smoking chamber. The CFD technique can be used to decrease aerosol concentration from Para rubber wood combustion. The study of particles concentration distribution on modification of the rubber smoking chamber by CFD technique field is very interesting in the future.

CONCLUSION

This review focuses on literature findings concerning RSS chamber of community-level rubber cooperatives in Thailand, RSS production process and monthly RSS production change, Particles size distribution and particles sampling method, PAHs concentration, the particles separation apparatuses reports and the decrease of the quantity smoke and soot particles by ventilation designed by computational fluid dynamics (CFD) technique. The following are the conclusions and recommendations from the review:

- RSS chamber of community-level rubber cooperatives in Thailand can be classified into two models: old and new model. The capacity of each chamber of new model (1995) is double in capacity of old model (1994).

- Fresh rubber latex is poured to tanks. Water and the acid are added to para-rubber latex to solidify the latex (tofu-like slabs). These slabs are then washed and squeezed to form thin layer sheets which have a thickness about 3-4 mm by a squeezing machine. Theses sheets are then hung on a cart and they are dried in a smoke chamber by hot gas from PR wood combustion. During the high season, the capacity of the factory is more than 15000 sheets per week and it has capacity about 7000-11000 sheets per week during the moderate season (Choosong et al., 2010).

- In the rubber smoking factory, smoke and soot particles from PR wood combustion contribute to pollution in the industry area, workplace and neighboring atmosphere. Smoke, soot, and PAHs concentration is very high for the furnace, chamber and workspace. Cascade impactors such as Andesen sampler are equipment for measuring the smoke and soot particles size distribution from para-rubber wood combustion. MMAD and GSD of smoke and soot particles were found to be 0.95 micron and 2.51, respectively (from Kalasee et al., 2003 report). But the report from Chomanee et al., 2009 presented that MMAD and GSD were found to be 0.68 micron and 3.04, respectively after improvement the air condensation.

- PAHs are emitted to an ambient air primarily from the incomplete of fuel combustion. PAHs had two types of poly-aromatic (PA) molecules: with and without side chain. PAHs compounds from Para rubber wood combustion were found 15 different PAHs components (Tekasakul et al., 2005; Furuuchi et al., 2006) and then able to be classified in two types: 2-3 rings and 4-6 rings (Chomanee et al., 2009).

- Three aerosol collecting techniques; filtration by stainless-wire mesh, inertial impaction (impaction wall) and ESP; are installed to remove the smoke and soot particles from the Para wood burning. This review indicates that the ESP installing between the furnace and the smoking chamber is suitable to eliminate aerosol particles at the rubber smoking industry. Ruttanachot et al. (2011) was improved ESPs technique of the earlier design by Kalasee (2009). Their result was shown that the collecting efficiency of ESPs was higher than 60%.

- CFD technique is used to study smoke and soot particles concentration, flow patterns, and particle motion. Modification of the ridge vents increased at roof of the rubber smoking chamber by CFD modeling and simulation could decrease the large particles concentration from the Para rubber wood combustion at the workplace and neighboring atmosphere (Purba & Tekasakul, 2012). In the future, CFD technique is very interesting method to improve the rubber smoking chamber. In addition to reduced the aerosol particles, CFD technique can be used to decrease the Para rubber wood consumption, energy decreased by a uniform velocity and temperature in the smoking chamber (Promtong & Tekasakul, 2007; Tekasakul & Promtong, 2008; Tanwanichkul et al., 2013; Dejchanchaiwong et al., 2014; Tekasakul et al., 2015; Dejchanchaiwong et al., 2016 and Dejchanchaiwong et al., 2017).

This review would be very helpful to the scientists and researchers who are learning and working on a field in the aerosol technology, the reduction of smoke and soot particles and PAHs concentration from Para rubber wood combustion, and improving the rubber smoking chamber by CFD technique.

Conflict of Interest

The authors declare no conflict of interest.

ACKNOWLEDGEMENTS

The authors thank King Mongkut's Institute of Technology Ladkrabang (KMITL), Prince of Chumphon Campus for giving an opportunity on this research.

REFERENCES

Adeola, A., Dena, M., John V. and Kerry, M. (2007). Environmental impact of polynuclear aromatic hydrocarbons: Extraction of polycyclic aromatic hydrocarbon (PAHs) from solid materials. Water Sci. & Tech., 11: 277-294.

Alonso, C., Olson, B., Goyal, S., Raynor, P., Davies, P. and Torremorell, M. (2017). Comparison of two size-differentiating air samplers for detecting airborne swine viruses under experimental conditions. Aerosol Sci. Technol., 51: 198–205.

Amuda, O. and Imeokparia, F. (2007). Polycyclic aromatic hydrocarbons in municipal waste ashes from three waste dumps in Lagos Nigeria. Chem. Soc. Ethiopia, 21: 141-144.

Andersen, A. (1956). Developmental work on the Andersen sampler. (Utah: Dugway Proving Ground Research Report).

ASTM E11, specifically governs the production of test sieves.

Bai, Y., Firuuchi, M., Tekasakul, P., Tekasakul, s., Choosong, T., Aizawa, M., Hata, M. and Otani, Y. (2007). Application of soft X-rays in the decomposition of polycyclic aromatic hydrocarbons

(PAHs) in smoke particles from biomass fuel burning. Aerosol Air Qual. Res. 7: 79–94.

Bharti, V., Gupta, B. and Kaur, J. (2019). Novel bacterial strains Pseudomonas sp. and Bacillus sp. isolated from petroleum oil contaminated soils for degradation of flourene and phenanthrene. Pollution, 5: 657-669.

Boussinesq, J. (1877). Theorie de l'Ecoulement Tourbillant, Mem. Presentes par Divers Savants Acad. Sci. Inst. Fr. 23: 46-50.

Butler, K. and Mulholland, G. (2004). Generation and transport of smoke components, Fire Technol., 40: 149–176.

Chaivatamaset, P. (2015). The defluidization during rubber wood combustion in fluidized bed. Inter. Energy. J. 15: 135-142.

Chao, C.Y.H., Kwong, P.C.W., Wang, J.H., Cheung, C.W. and Kendall, G. (2008). Co-firing coal with rice husk and bamboo and the impact on particulate matters and associated polycyclic aromatic hydrocarbon emissions. Bioresour. Technol. 99: 83-93.

Cheng, Y., Zhou, Y., Irvin, C., Kirkpatrick, B. and Backer, L. (2007). Characterization of aerosols containing microcystin. Mar. Drugs. 5: 136-150.

Chomanee, J., Tekasakul, S., Tekasakul, P., Furuuchi, M. and Otani, Y. (2009). Effects of moisture content and burning period on concentration of smoke particles and particle-bound polycyclic aromatic hydrocarbons from rubber-wood combustion. Aerosol Air Qual. Res. 9: 404–411.

Choosong, T., Furuuchi, M., Tekasakul, P., Tekasakul, S., Chomanee, J., Jinno, T., Hata, M. and Otani, Y. (2007). Working environment in a rubber sheet smoking factory polluted by smoke from biomass fuel burning and health influences to workers. J. Ecotechnol. Res. 13: 91-96.

Choosong, T., Chomanee, J., Tekasakul, P., Tekasakul, S., Otani, Y., Hata, M. and Furuuchi, M. (2010). Workplace environment and personal exposure of PM and PAHs to workers in natural rubber sheet factories contaminated by wood burning smoke. Aerosol Air Qual. Res. 10: 8-21.

Croft, B., Martin, R., Leaitch, W., Tunved, P., Breider, T., D'Andrea, S. and Pierce, J. (2016). Processes controlling the annual cycle of Arctic aerosol number and size distributions, Atmos. Chem. Phys., 16: 3665–3682.

Davies, C. (1952). The separation of airborne dust and mist particles. Proc. Inst. Mech. Engr. 1B: 185-198.

Davies, C. (1966). Aerosol science. (London: Academic Press)

Dejchanchaiwong, R., Tirawanichakul, Y., Tirawanichakul, S. and Tekasakul, P. (2014). Single-phase and multi-phase models for temperature and relative humidity calculations during forced convection in a rubber-sheet drying chamber, Maejo Int. J. Sci. Tech. 8: 207–220.

Dejchanchaiwong, R., Arkasuwan, A., Kumar, A. and Tekasakul, P. (2016). Mathematical modeling and performance investigation of mixed-mode and indirect solar dryers for natural rubber sheet drying. Energy Sustainable Dev. 34: 44–53.

Dejchanchaiwong, R., Tirawanichakul, Y., Tirawanichakul, S., Kumar, A. and Tekasakul, P. (2017). Conjugate heat and mass transfer modeling of a new rubber smoking room and experimental validation, Appl. Therm. Eng. 112: 761-770

Deng, H., Pingan, P. and Jianzhong, W.H. (2006). Distribution and loadings of polycyclic aromatic hydrocarbons in the Xijiang River in Guangdong, South China. J. Chem., 64: 1401-1411.

Docherty, K., Wu, W., Lim, Y., Ziemann, P. (2005). Contributions of organic peroxides to secondary aerosol formed from reactions of monoterpenes with O_3. Environ. Sci. Technol. 39: 4049–4059.

Donde, P., Raman, V., Mueller, M.E., Pitsch, H. (2013). LES/PDF based modeling of soot-turbulence interactions in turbulent flames. Proc. Combust. Inst. 34: 1183–1192

Fang, G., Wu, Y., Chen, M., Ho, T., Huang, S., and Rau, J. (2004). Polycyclic aromatic hydrocarbons study in Taichung, Taiwan, during 2002-2003, Atm. Environ., 38: 3385-3391.

Fenklach, M. and Wang, H. (1991). Aromatics growth beyond the first ring and the nucleation of soot particles, Div. Fuel Chem., 36: 1509

Friedlander, S. (2000). Smoke, dust, and haze: fundamentals of aerosol dynamics. (Oxford: Oxford University Press Inc.)

Fuchs, N. A. (1947). The charges on the particles of aerocolloids. Investiya Acad. Nauk USSR, Ser. Geogr. Geophys. 11:341.

Furuuchi, M., Tekasakul, P., Murase, T., Otani, Y., Tekasakul, S. and Bai, Y. (2006). Characteristics of particulates emitted from rubber-wood burning. J. Ecotechnol. Res. 12: 135–139.

Giechaskiel, B., Maricq, M., Ntziachristos, L., Dardiotis, C. Wang, X., Axmann, H., Bergmann, A. and Schindle, W. (2014). Review of motor vehicle particulate emissions sampling and measurement: From smoke and filter mass to particle number. J. Aerosol Sci. 67: 48-86.

Gras, J. and Michael, C. (1979). Measurement of the stratospheric aerosol particle size distribution. J. App. Meteorol. 18: 855-860.

Haider, A., and Levenspiel, O. (1989). Drag coefficient and terminal velocity of spherical and non-spherical particles. Powder Tech. 58: 63–70.

Hata, M., Chomanee, J., Thongyen, T., Bao, L., Tekasakul, S., Tekasakul, P., Otani, Y. and Furuuchi, M. (2014). Characteristics of nanoparticles emitted from burning of biomass fuels. J. Environ. Sci. 26: 1913-1920.

Hinds, W.C. (1999) Aerosol Technology. (New York: John Wiley & Sons)

Homann, K. H. and Wagner, H. Gg. (1966). Paper presented at the 11th. International on Combustion, The Combustion Institute, Pittsburgh, pp. 371–379.

Intra, P. and Tippayawong, N. (2005). Approach to characterization of a diode type corona charger for aerosol size measurement. KIEE Int. Trans. Electrophysics App. 5-C: 196–203.

Intra, P. and Dussadee, N. (2007). Approach to predict the total collection efficiency of a wire-plate electrostatic precipitator for particles removal from biomass furnace. (Paper presented at the 21st. Conference of Mechanical Engineering Network of Thailand, Chonburi, Thailand, pp. 152–158)

Intra, P., Limueadphai, P. and Tippayawong, N. (2010). Particulate emission reduction from biomass burning in small combustion systems with a multiple tubular electrostatic precipitator. Part. Sci. Technol. 28: 547–565.

Intra, P. and Tippayawong, N. (2011). An overview of unipolar developments for nanoparticle charging. Aerosol Air Qual. Res. 11: 187–209.

ISO 3310-1:2016. Test sieves-technical requirements and testing, Part 1: Test sieves of metal wire cloth.

JB/T 12591-2016. Low-low temperature electrostatic precipitator

Kalasee, W., Tekasakul, S., Otani, Y. and Tekasakul, P. (2003). Characteristic of soot particles produced from rubber wood combustion. (Paper presented at the 2nd. Asian Particle Technology Symposium, Penang, Malaysia, pp. 103–108).

Kalasee, W., Pongpariyawatee, Y., Tantaprapa, W., Suwanjarat, S., Kirirat, P. and Tekasakul, P. (2003). Fuel efficiency enhancement in the rubber smoking process of the rubber cooperatives. (Paper presented at the 17th. Conference of Mechanical Engineering Network of Thailand, Prachinburi, Thailand, pp. 560-564).

Kalasee, W. (2009). Improvement soot particles separation equipments for rubber smoking chamber. Aerosol Air Qual. Res. 9: 333–341.

Kalasee, W., Thungsotanon, D., Srisang, N. and Daungwilailux, P. (2012). The Effect of Wood Vinegar Concentration on the Quality of Rubber Sheets. (Paper presented at the 13th. Annual Conference of Thai Society of Agricultural Engineering, Chiang Mai, Thailand, pp. 557-565).

Kanaoka, C., Furuuchi, M., Myojo, T., Inaba, J. and Ohmata, K. (2006). Numerical investigation of flow and dust concentration distributions in the work area of a mountain tunnel currently under construction. Aerosol Air Qual. Res. 6: 231–246.

Kesavan, J., Kesavan, M. and Rule, A. (2017). Sampling efficiencies of two modified viable cascade impactors. Aerosol Sci. Technol., 51: 1296–1302.

Keyte, I.J., Harrison, R.M. and Lammel, G. (2013). Chemical reactivity and long-range transport potential of polycyclic aromatic hydrocarbons--A review, Chem. Soc. Rev. 42: 9333–9391

Kihm, K. (1987). Effects of Non-uniformities on Particle Transport in Electrostatic Precipitators, Dissertation, Stanford University

Kim, S. and Lee, K. (1999). Experimental study of electrostatic precipitator performance and comparison with existing theoretical prediction models, J. Electrost. 48: 3–25.

Kim, C., Noh, K.C. and Hwang, J. (2010). Numerical investigation of corona plasma region in negative wire-to-duct corona discharge, Aerosol Air Qual. Res. 10: 446–455

Kocik, M., Dekowski, J., Mizeraczyk, J. (2005). Particle precipitation efficiency in an electrostatic precipitator. J. Electrostat. 63: 761–766.

Kuarsakul, N., Ruangwong, B. and Pewpuak, P. (2011). Study of entrapping powder by electrostatic precipitator, Dissertation, King Mongkut's Institute of Technology Ladkrabang, Prince of Chumphon Campus, Chumphon, Thailand

Letts, G.M., Raynor, P.C. and Schumann, R.L. (2003). Selecting fiber materials to improve mist filters, J. Aerosol Sci. 34: 1481-1492

Lewis, D.A. and Copley, M. (2011). Inhaled product characterization: Calculating particle-size distribution Metrics, Pharm. Technol. 35: 33–37

Lin, C., Lin, L., Hong, M., Zhang, J., Yong, D. and Chun, M. (2011). Analysis of the scale characteristics in salt sludge wet FGD system. J. China. Coal. Soc., 36: 1554–1558

Lin, C., Yue, L., Yuzhou, T., Yifei, S., Qingsong, W., Xueliang, Y. and Jon, K. (2018). Integrated assessment of the environmental and economic effects of an ultra-clean flue gas treatment process in coal-fired power plant, J. Clean. Prod., 199: 359–368.

Long, Z. and Yao, Q. (2010). Evaluation of various particle charging models for simulating particle dynamics in electrostatic precipitators. J. Aerosol. Sci., 41: 702–718.

Loomans, M. and Lemaire, T. (2002) Particle concentration calculations using CFD - a Comparison. (Paper presented at the Conference of Indoor Air, Edinburgh, Scotland, pp.153-156).

Lu, W., Howarth, A.T., Adam, N. and Riffat, S.B. (1996). Modelling and measurement of airflow and aerosol particle distribution in a ventilated two-zone chamber, Building Environ., 31: 417-423.

Ma, S., Chai, J., Chen, G., Yu, W. and Zhu, S. (2016). Research on desulfurization wastewater evaporation: present and future perspectives, Renew. Sustain. Energy Rev., 58: 1143–1151.

Mahmudi, M., Hashemi, S. and Salemi, A. (2019). A multi-metric index for hydrocarbons source apportionment, Pollution, 5: 419-427

Martinis, D., Okamoto, A., Kado, N., Gundel, A. and Carvalho, R.F. (2002). Polycyclic aromatic hydrocarbons in a bioassay fractionated extract of PM10 collected in Sao Paulo, Brazil, Atmos. Environ. 36: 307-314.

Matiyanon, T., Sathitreaungsuk, P. and Sangworakran, S. (2013). Design and performance evolution of furnace and rubber-smoked sheet (RSS) drying system high-efficiency. (Paper presented at the 27th. Conference of Mechanical Engineering Network of Thailand, Prachinburi, Thailand)

Matiyanon, T., Sathitreaungsuk, P., Sangworakran, S.and Boonprasit, P. (2014). Design and experiment of an energy-saving combustor equipped with a multi-pass heat exchanger for a high-efficiency rubber-smoked system. (Paper presented at the 28th. Conference of Mechanical Engineering Network of Thailand, Khon Kaen, Thailand)

Mc Murry, J. (2000). Organic chemistry. (USA: Brooks/Cole).

Motamedimehr, S. and Gitipour, S. (2019). Extraction and recovery of polycyclic aromatic hydrocarbons in petroleum contaminated soils using supercritical water by response surface methodology. Pollution, 5: 913-922.

Park, J.W., Kim, C., Park, J. and Hwang, J. (2018). Computational Fluid Dynamic Modelling of Particle Charging and Collection in a Wire-to-Plate Type Single-Stage Electrostatic Precipitator, Aerosol Air Qual. Res. 18: 590–601.

Parker, K.R. (1997). Applied Electrostatic Precipitation. (New York: Blackie Academic & Professional).

Phairuang, W., Tekasakul, P., Hata, M., Tekasakul, S., Chomanee, J., Otani, Y. and Furuuchi, M. (2019). Estimation of Air Pollution from Ribbed Smoked Sheet Rubber in Thailand exports to Japan as a Pre-Product of Tires. Atmos. Poll. Res. 10: 642-650.

Phonchat, T. and Choowijit, T. (2011). A Study of The Particle Distribution in Atmosphere, Dissertation, King Mongkut's Institute of Technology Ladkrabang, Prince of Chumphon Campus, Chumphon, Thailand.

Promtong, M. (2006). CFD Study of Flow in Rubber Smoking Room and Modification to Improve Uniformity of Velocity and Temperature Distributions, Master of Engineering Thesis in Mechanical Engineering, Prince of Songkla University, Songkhla, Thailand.

Promtong, M. and Tekasakul, P. (2007). CFD Study of Flow in Rubber Smoking-room: I. Validation with the Present Smoking-room, Appl. Therm. Eng. 27: 2113-2121.

Purba, L. (2009). Airflow and Aerosol Concentration in a Ribbed Smoked Sheet Rubber Cooperative and Improvement of Ventilation, Dissertation, Prince of Songkla University, Songkhla, Thailand.

Purba, L. and Tekasakul, P. (2012). Computational Fluid Dynamics Study of Flow and Aerosol Concentration Patterns in a Ribbed Smoked Sheet Rubber Factory, Particulate Sci. Tech. 30: 220-237.

Raman, V. and Fox, R. (2016). Modeling of fine-particle formation in turbulent flames. Annu. Rev. Fluid Mech. 48: 159–190.

Rattanamechaiskul, C., Junka, N., Potichalung, J., Wingwon, T., Boontum, W. and Srisang, N. (2016). Whiteness index Prediction of Para Rubber Sheet during Hot Air Drying. KKU Eng. J. 43: 331-333.

Riahi, S., Beyler, C. and Hartman, J. (2013). Wall smoke deposition from a hot smoke layer. Fire Technol., 49: 395–409.

Ravindra, K., Bencs, L., Wauters, E., de Hoog, J., Deutsch, F., Roekens, E., Bleux, N., Bergmans, P., and Van Grieken, R. (2006). Seasonal and site specific variation in vapor and aerosol phase PAHs over Flanders (Belgium) and their relation with anthropogenic activities. Atm. Environ., 40: 771- 785.

Rigopoulos, S. (2010). Population balance modelling of poly-dispersed particles in reactive flows, Prog. Energy Combust. Sci. 36: 412–443

Rigopoulos, S. (2019). Modelling of soot aerosol dynamics in turbulent flow, Flow Turbulence Combustion, 103: 565–604

Ruttanachot, C., Tirawanichakul, Y. and Tekasakul, P. (2011). Application of Electrostatic Precipitator in Collection of Smoke Aerosol Particles from Wood Combustion. Aerosol Air Qual. Res. 11: 90–98.

Saez, F., Cabanas, A., Gonzalez, A., Murillo, J.M., Martinez, J.M., Rodriguez, J.J and Dorronsoro, J.L. (2003). Cascade Impactor Sampling to Measure Polycyclic Aromatic Hydrocarbons from Biomass Combustion Processes. Biol. Eng. 86: 103-111.

Salaudeen, I., Sonibare, O., Sojinu, S. and Ekundayo, O. (2017). Polycyclic aromatic hydrocarbons in air from industrial areas in Lagos and Ogun states, Nigeria. Pollution, 3: 561-573.

Satcher, M. (1995). Toxicological profile for polycyclic aromatic hydrocarbons. Agency for Toxic Substances and Disease Registry, Atlanta, Georgia: 1-457.

Shin, T., Kazuhiko, N., Makoto, S. and Hisao, H. (1988). Determination of benzo[a] pyrene in airborne particulates by automated thermal desorption gaschromatography. Anal. Sci., 4: 115-116.

Simonelt, B., Sheng, G., Chen, X., Fu, J., Zhang, J., and Xu, Y. (1991). Molecular marker study of extractable organic matter in aerosols from urban areas of China. Atm. Environ., 25: 2111-2129.

Sippola, M. (2002). Particle deposition in ventilation ducts. Ph.D. thesis, University of California, Berkeley

Sippola, M. and Nazaroff, W. (2010). Experiments measuring particle deposition from fully developed turbulent flow in ventilation ducts. Aerosol Sci. Technol., 38: 914–925.

Sirisantipong, T. and Tantichaowanan, M. (2002). Pressure drop evolution of a medium-performance fibrous filter, Bachelor of Science Project in Physical Chemistry, Prince of Songkla University, Songkhla, Thailand

STP555, Instrumentation for Monitoring Air Quality.

STP1002, Design and Protocol for Monitoring Indoor Air Quality.

STP1287, Characterizing Sources of Indoor Air Pollution and Related Sink Effects.

Tanaka, Y. (2003). Mass transport and energy consumption in ionexchange membrane electro-dialysis of seawater, J. Membr. Sci., 215: 265–279.

Tanaka, Y. (2006). Irreversible thermodynamics and overall mass transport in ion-exchange membrane electro-dialysis, J. Membr. Sci., 281:517– 531.

Tang, N., Hattori, T., Taga, R., Igarashi, K., Yang, X., Tamura, K., Kakimoto, H., Mishukov, V. F., Toriba, A., Kizu, R. and Hayakawa, K. (2005). Polycyclic aromatic hydrocarbons and Nitropolycyclic aromatic hydrocarbons in urban air particulates and their relationship to emission sources in the Pan-Japan sea countries, Atmos. Environ., 39: 5817-5826

Tantichaowanan, M. (2005). Performance of an electrostatic precipitator designed for collection of soot Particles from wood combustion, Dissertation, Prince of Songkla University, Songkhla, Thailand.

Tanwanichkul, B., Thepa, S. and Rordprapat, W. (2013). Thermal modeling of the forced convection sandwich greenhouse drying system for rubber sheets, Energy Convers. Manage. 74: 511–523.

Tekasakul, P., Tekasakul, S., Tantichaowanan, M., Kalasee, W. and Otani, Y. (2005). Removal of smoke particles produced from rubberwood combustion in rubber smoking industry. (Paper presented at the 4th. Asian Aerosol Conference, Mumbai, India, pp. 677–678).

Tekasakul, S., Tantichaowanan, M., Otani, Y., Kuruhongsa, P. and Tekasakul, P. (2006). Removal of soot particles in rubber smoking chamber by electrostatic precipitator to improve rubber sheet Color, Aerosol Air Qual. Res. 6: 1-14.

Tekasakul, P. and Promtong, M. (2008). Energy efficiency enhancement of natural rubber smoking process by flow improvement using a CFD technique, Appl. Energy 85: 878–895.

Tekasakul, P., Furuuchi, M., Tekasakul, S., Chomanee, J. and Otani, Y. (2008), Characteristics of PAHs in particles in the atmospheric environment of Hat Yai city, Thailand, and relationship with rubber-wood burning in rubber sheet production, Aerosol Air Qual. Res. 8: 265-278.

Tekasakul, S., Suwanwong, P., Otani, Y. and Tekasakul, P. (2008), Pressure drop evolution of a medium-performance fibrous filter during loading of mist aerosol particles, Aerosol Air Qual. Res. 8: 348-365

Tekasakul, P., Dejchanchaiwong, R., Tirawanichakul, Y. and Tirawanichakul, S. (2015). Three dimensional numerical modeling of heat and moisture transfer in natural rubber sheet drying process, Dry. Tech. 33: 1124–1137.

Thailand Rubber Research Institute, Department of Agriculture, Ministry of Agriculture and Cooperatives, Retrieved 2017, from http:///www.rubberthai.com

Thailand Rubber Research Institute, Department of Agriculture, Ministry of Agriculture and Cooperatives, Retrieved 2018, from http:///www.rubberthai.com

Tian, Z. F., Tu, J. Y. and Yeoh, G. H. (2007). CFD studies of indoor airflow and contaminant particle transportation, Particulate Sci. Tech. 25: 555–570.

Venkataraman, C., Negi, G., Sardar, S.B. and Rastogi, R. (2002). Size distributions of polycyclic aromatic hydrocarbons in aerosol emissions from biofuel combustion, J. Aerosol Sci. 33: 503-518.

Wang, Y., Li, P., Hong-li, L., Xiao, L., and Wen, W. (2010). PAHs distribution in precipitation at Mount Taishan China. Identification of sources and meteorological influences, Atm. Resear. 95: 1-7.

White, H. J. (1951). Particle charging in electrostatic precipitation, *Trans. Am. Inst. Elec. Engrs.* 70:1186–1191.

White, H.J. (1963). Industrial electrostatic precipitation. (Massachusettes: Addison-Wesley).

Zhang, Z. and Chen, Q. (2006). Experimental measurements and numerical simulations of particle transport and distribution in ventilated rooms, Atmos. Environ., 40: 3396-3408.

Zhao, S., Duan, Y., Lei, C., Li, Y., Yao, T., Shuai, L., Meng, L. and Lu, J. (2017). Study on emission of hazardous trace elements in a 350 MW coal-fired power plant. Mercury. Environ Pollut., 229: 863–870.